

Theoretical study on *p*-type dyes with different π -linkers for dye-sensitized solar cells

X. H. LI^a, W. YAN^b, Q. Y. Xia^{c,*}, X. H. JU^{b,*}

^aCollege of Physics and Engineering, Henan University of Science and Technology, Luoyang, 471003, China

^bKey Laboratory of Soft Chemistry and Functional Materials of MOE, School of Chemical Engineering, Nanjing University of Science and Technology, Nanjing 210094, P. R. China.

^cSchool of Chemistry and Chemical Engineering, Linyi University, 276005 Linyi, P. R. China

The triphenylamine-based dyes were designed as the *p*-type sensitizers. The absorption spectra, electronic transitions, electronic structures of the sensitizers were systematically studied. The absorption bands of **O2-C** and **O2-D** are red-shifted and have broad band in the visible light area at 524 nm and 559 nm, respectively, compared to their prototype **O2**. Both ΔG_{inj} and ΔG_{reg} values for all the designed dyes are in range of -3.04 to -4.13 eV and -1.08 to -2.68 eV, respectively, which is good for hole injection and dye regeneration. The positive ΔG_{CR} values could reduce charge recombination which is benefit for charge transferring from the donor to the acceptor. Importantly, dyes **O2-C** and **O2-D** are predicted to be promising candidates for the *p*-type sensitizers in comparison with prototype **O2**.

(Received January 31, 2019; accepted February 17, 2020)

Keywords: Dye sensitized solar cells (DSSCs), Triphenylamine-based D- π -A dye, *p*-Type sensitizers, Density functional theory, Absorption spectrum

1. Introduction

Solar energy has owned extensive attention for it is environment-friendly and has the potential for sustainable development [1]. The study of photovoltaic solar cell which can convert solar energy to chemical energy available to humans is popular. Early solar cells investigated by Grätzel and coworkers achieved 7.1% conversion efficiency [2]. Later, higher efficiency of 13% was achieved with dye-sensitized solar cell (DSSC) [3]. Further, inexpensive metal complexes and full organic dyes such as triarylamine-based [4] had also been investigated for DSSCs. However, the development lag of *p*-type DSSCs clipped the wings of the high-efficiency tandem *pn*-DSSCs. Therefore, the improvement of *p*-type DSSCs is high on the agenda [5].

Density functional theory (DFT) and time-dependent (TD) DFT methods are widely employed for the molecular structure calculation in DSSCs. What's more, the first line of the theoretical study is the rational design of molecular structures. Donor- π -linker-Acceptor (D- π -A) is the typical configuration of sensitizers [6-7]. Recently, Li et al investigated triphenylamine-based *p*-type organic dyes with different π -linkers [8]. Zhang and coworkers compared different electron-induced effects in *p*-type dyes with theoretical calculation [9]. Therefore, we choose triphenylamine as the donor, formic acid as the anchor, 2-methylenemalononitrile as the acceptor, and different π -linkers are inserted between the donor and

acceptor.

Based on above discussion, we chose O2 as the prototype and designed a series of novel triarylamine structures in the form of D- π -A chain (Fig. 1). we designed **O2-A** to **O2-E** with 1-ethyl-4-methyl-2,5-dihydro-1H-1,2,3-triazole, 1,3,4-oxadiazole, benzo[c][1,2,5]thiadiazole, 4-(thiophen-2-yl)benzo[c][1,2,5]thiadiazole, 4-(1,3,4-oxadiazol-2-yl)benzo[c][1,2,5]thiadiazole as π -linker, respectively.

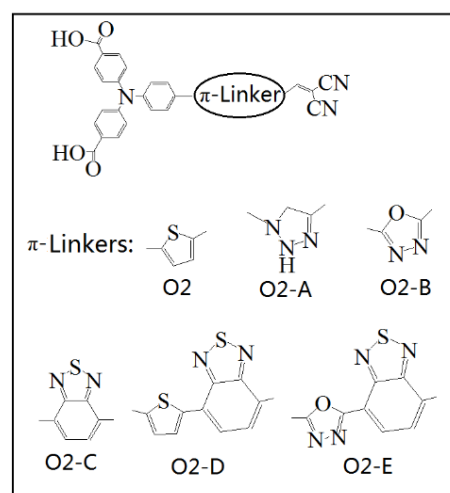


Fig. 1. Dye structures and their linkers

2. Methods and computation details

As is known to all, the *p*-type dyes with high light harvesting efficiency (LHE), hole injecting efficiency (HJE), dye regeneration efficiency (DRE) but low charge recombination efficiency (CRE) would be high efficient. The LHE is related to oscillator strength (*f*) with the counterpart of λ_{\max} can be expressed as following equations [10]:

$$\text{LHE} = 1 - 10^{-f} \quad (1)$$

The free energy (in eV) of HJE, DRE, CRE are expressed as ΔG_{inj} , ΔG_{reg} and ΔG_{CR} respectively. The relevant equations are [11]:

$$\Delta G_{\text{inj}} = E_{\text{VB}} - (E_{0-0}(\text{dye}^*) + E_{\text{red}}(\text{dye})) \quad (2)$$

$$\Delta G_{\text{reg}} = E(I_3^-/I^-) - E_{\text{red}}(\text{dye}) \quad (3)$$

$$\Delta G_{\text{CR}} = E_{\text{VB}} - E(\text{dye}/\text{dye}^-) \quad (4)$$

where E_{VB} is the valence band (VB) potential of semiconductor, $E_{0-0}(\text{dye}^*)$ is the vertical transition energy of sensitizer, $E(\text{dye}/\text{dye}^-)$ represents reduction potential of sensitizer, $E(I_3^-/I^-)$ means reduction potential of redox mediator.

All the calculations were performed in Gaussian 09W package [12]. Several functionals of B3LYP, CAM-B3LYP, LC-BLYP, MPW1K, PBE0 were tested to choose a better functional [8, 13]. It can be found that the model results calculated in CAM-B3LYP/6-31G(d,p) combined with polarized continuum model in solvent DMF approaches to the experimental values for this system [14]. What's more, all the dyes were calculated by the TD-DFT method.

3. Results and discussion

3.1. Electronic structures

The electronic distribution of HOMO and LUMO for the optimized *p*-type structures **O2** and its remodeled dyes **O2-A**–**O2-E** are displayed in Fig. 2. From the figure, we can see that all the highest occupied molecular (HOMO) are below the valence band ($E_{\text{VB}} = -4.98$ eV) of the semiconductor NiO, which guarantees sufficient hole injection. Furthermore, the value of the lowest unoccupied molecular orbital (LUMO) are above of the value of electrolyte ($E(I_3^-/I^-) = -4.80$ eV), which guarantees the dye regeneration smoothly. For structures **O2-A** to **O2-E**, the HOMO levels decrease in the order of **O2-D**, **O2-C**, **O2-E**, **O2-B** and **O2-A**. The introduction of 1,4-dimethyl-2,5-dihydro-1H-1,2,3-triazole and 1,3,4-oxadiazole can reduce the HOMO

energy level which is good for hole injection from the VB of the semiconductor NiO to the HOMO of the dye. What's more, the LUMO levels of structure **O2-B**, **O2-C**, **O2-D**, **O2-E** are lower than that of the prototype **O2**.

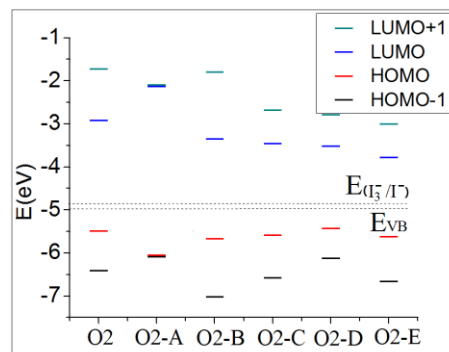


Fig. 2. The frontier molecular orbital energy levels for studied dyes in DMF solvent at PCM-B3LYP/6-31G(d,p) level (color online)

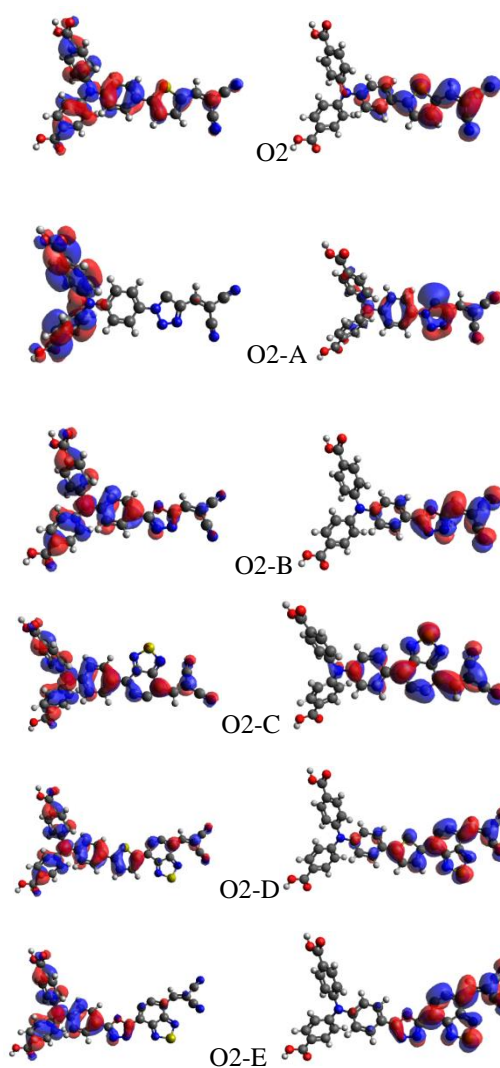


Fig. 3. HOMO (left) and LUMO (right) of **O2** and its modified dyes (color online)

From Fig. 3, we can see that the electron distribution of HOMO in structure **O2-A** is dominantly distributed on the donor (triphenylamine) which is close to the anchoring group. Whereas for structures **O2-B**, **O2-C**, **O2-D** were mainly delocalized over not only the donor but also part of π -linkers. The LUMOs distributions of all the structures have more overlap with the acceptors which can reduce the charge recombination [15]. Structure **O2-A** are more in favor of hole injection than other structures because its HOMOs and LUMOs hardly overlap with each other, and therefore a rapid hole injection and low charge recombination are guaranteed [16]. The structures with 1,4-dimethyl-2,5-dihydro-1H-1,2,3-triazole as π -linker shows better performance in hole injection.

3.2. UV/vis absorption spectra

The absorption spectrum of the sensitizers is the most vital factor to estimate whether the *p*-type DSSCs is efficient or not. Therefore, it is important to select an appropriate functional to simulate the UV/vis absorption spectrum of the dyes. We take **O2** as the prototype, common functionals such as B3LYP, CAM-B3LYP, LC-BLYP, MPW1K, PBE0 were tested and the results were collected in Table 1. The λ_{\max} of prototype **O2** calculated by CAM-B3LYP (428 nm) are more comparable to the experimental value (423 nm), indicating the CAM-B3LYP is more suitable to simulate the performance of the dyes although its ϵ value is not as good as those from other functionals. In evaluating the suitability of theoretical method in the benchmark calculations, the maximum adsorption wavelength of an efficient dye for sunlight harvesting is more important than the ϵ value, as long as the ϵ value is large enough. The adsorption wavelength is related to the energy difference in the electron transition process. If a method fails to predict this property, it will be unsuitable for investigating the optoelectronic properties even if it predicts the ϵ value well. Thus, all the structures were investigated at CAM-B3LYP/6-31G(d,p) level in DMF.

Table 1. Calculated absorption spectra of **O2** in DMF by different functionals

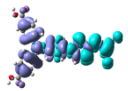
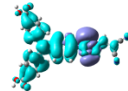
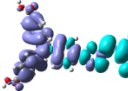
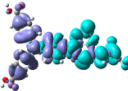
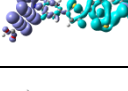
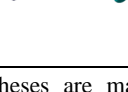
Functionals	λ_{\max} (nm)	$\Delta\lambda$ ^a	ϵ ^b	$\Delta\epsilon$ ^c
(Expt.)	423	—	2.897	—
B3LYP	548	125	3.692	0.975
CAM-B3LYP	428	5	6.18	3.27
PBE0	440	17	5.373	2.476
MPW1K	440	17	5.197	2.282

^a $\Delta\lambda = |\lambda_{\text{exp}} - \lambda_{\text{cal}}|$ (nm). ^b ϵ ($\times 10^4 \text{ M}^{-1} \text{ cm}^{-1}$). ^c $\Delta\epsilon = |\epsilon_{\text{exp}} - \epsilon_{\text{cal}}|$ ($\times 10^4 \text{ M}^{-1} \text{ cm}^{-1}$)

The major excitation energies, oscillator strengths,

maximum absorbance wavelengths, main configurations and equivalent MO transitions were listed in Table 2. The λ_{\max} of **O2-C** and **O2-D** red-shift to 524 nm and 559 nm, respectively, compared to prototype **O2**. Their corresponding oscillator strengths (f) are as high as 1.52 and 1.92, respectively, which may guarantee large sunlight harvesting. These two structures could be good dye candidates. Moreover, the percentages of electron transitions of all the dyes from HOMO to LUMO are all above 77% except **O2-E**. It also can be seen that the electron density difference maps of $S_0 \rightarrow S_1$ for **O2-D** has the least charge density overlap between donor and acceptor, which is in favor of charge separation.

Table 2. Computed maximum absorption wavelengths (λ_{\max}/nm), oscillator strengths (f), transition configurations and the electron density difference maps of **O2**, **O2-A**–**O2-E** corresponding to $S_0 \rightarrow S_1$

Syst em	E(e V)	$\lambda_{\text{m ax}}$ (nm)	f	Main Configurations ^a	$S_0 \rightarrow S_1$ ^b
O2	2.57	428	1.52	H-1 \rightarrow L (16%) H \rightarrow L (78%) H \rightarrow L+2 (3%)	
O2-A	1.27	345	0.49	H-1 \rightarrow L (12%) H \rightarrow L (77%) H \rightarrow L+1 (8%)	
O2-B	2.31	407	1.10	H-1 \rightarrow L (12%) H \rightarrow L (77%) H \rightarrow L+1 (8%)	
O2-C	2.13	524	1.52	H \rightarrow L (89%) H-1 \rightarrow L (7%)	
O2-D	1.92	559	1.80	H \rightarrow L (89%) H-1 \rightarrow L (7%)	
O2-E	1.84	473	1.24	H-1 \rightarrow L (28%) H \rightarrow L (66%) H \rightarrow L+3 (4%)	

^a H-1 means HOMO-1, and data in parentheses are main configuration contributions. ^b $S_0 \rightarrow S_1$ means an electronic excitation to the first singlet state. The purple and green colors represent a decrease and increase of charge densities, respectively.

The calculated absorption spectra of **O2** and all the remodeling structures were shown in Fig.4. We can see all the structures have two absorption bands except for **O2** and **O2-C** having three. Compared with **O2**, the maximum absorption wavelengths of **O2-C** and **O2-D** red-shift and have more overlap with the visible light. For the designed structures, the maximum absorption wavelengths increase in order: **O2-D** (559 nm) > **O2-C** (524 nm) > **O2-E** (473 nm) > **O2** (428 nm) > **O2-B** (407 nm) > **O2-A** (345 nm). The maximum absorption bands of the dyes are originated by the electron transfer from the HOMO to the LUMO, which is benefit to the hole injection.

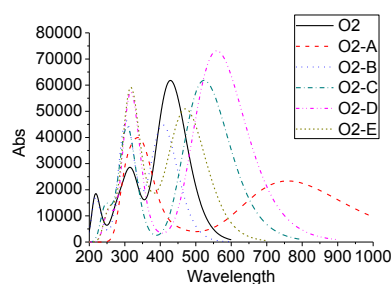


Fig. 4. Absorption spectra of **O2**, **O2-A**–**O2-E** (color online)

3.3. The performance of dyes in DSSCs

Based on the theory mentioned above, the calculated *LHE*, ΔG_{inj} , ΔG_{reg} , ΔG_{CR} are showed in Table 3. As we can see, the *LHE* value of **O2-D** is the larger than prototype **O2**, indicating that the former has higher light harvesting efficiency. While **O2-C** is the same as **O2**. In addition, the redox potentials of all the dyes are also calculated and analyzed. Both ΔG_{inj} and ΔG_{reg} are negative, which is good for hole injection and dye regeneration. And the ΔG_{inj} and ΔG_{reg} values of **O2-C** (−3.66 and −1.35, respectively) is more negative than those of **O2-D** (−3.39 and −1.29, respectively). For ΔG_{CR} , all the values are positive which can hinder the charge recombination. Therefore, inserting benzo[c][1,2,5]thiadiazole and 4-(thiophen-2-yl)benzo[c][1,2,5]thiadiazole can effectively improve the dye performance by modifying the energy level and the absorption performance of the structures.

Table 3. Computed *LHE*, $E_{0-0}(dye^*)$, $E_{red}(dye)$, ΔG_{inj} , ΔG_{reg} and ΔG_{CR} of dyes **O2**, **O2-A** to **O2-E**^a

System	<i>LHE</i>	$E_{0-0}(dye^*)$	$E_{red}(dye)$	ΔG_{inj}	ΔG_{reg}	ΔG_{CR}
O2	0.970	2.57	2.92	−4.63	−1.88	2.06
O2-A	0.676	1.27	2.12	−4.13	−2.68	2.86
O2-B	0.921	2.31	3.35	−3.94	−1.45	1.63
O2-C	0.970	2.13	3.45	−3.66	−1.35	1.53
O2-D	0.984	1.92	3.51	−3.39	−1.29	1.47
O2-E	0.942	1.84	3.78	−3.04	−1.02	1.20

^a *E* and ΔG are in eV.

4. Conclusion

In this work, several functionals were tested and we chose the most suitable one. The prototype and designed dyes were calculated by CAM-B3LYP in solvent DMF. We designed the new structures by replacing the π -linker of prototype **O2** (thiophene). Judged from the properties of all the p-type dyes we calculated above, **O2-C** and **O2-D** with the π -linkers of benzo[c][1,2,5]thiadiazole, 4-(thiophen-2-yl)benzo[c][1,2,5]thiadiazole have better performance than prototype **O2** with satisfied electronic structures, larger absorption overlap with visible light, high *LHE* and effective ΔG_{inj} , ΔG_{reg} and ΔG_{CR} .

Acknowledgments

W. Yan thanks the Innovation Funding from the Graduate School of NJUST (No. SJLX16_0140) for partial supporting of this work.

References

- [1] W. Wu, J. Zhang, K. Xu, Y. Qu, H. Zhu, *Sustainability* **9**, 726 (2017).
- [2] B. O'Regan, M. Grätzel, *Nature* **353**, 727 (1991).
- [3] S. Mathew, A. Yella, P. Gao, R. Humphry-Baker, B. F. E. Curchod, N. Ashari-Astani, I. Tavernelli, U. Rothlisberger, M. K. Nazeeruddin, M. Grätzel, *Nat. Chem.* **6**, 242 (2014).
- [4] X. F. Ren, G. J. Kang, Q. Q. He, *J. Mol. Model.* **22**, 8 (2016).
- [5] L. Li, E. A. Gibson, P. Qin, G. Boschloo, M. Gorlov, A. Hagfeldt, L. Sun, *Adv. Mater.* **22**, 1759 (2010).
- [6] Z. Huang, G. Natu, Z. Ji, M. He, M. Yu, Y. Wu, *J. Phys. Chem. C* **116**, 26239 (2012).
- [7] H. B. Li, J. Zhang, Y. Wu, J. L. Jin, Y. A. Duan, Z. M. Su, Y. Geng, *Dyes Pig.* **108**, 106 (2014).
- [8] N. Nasr, M. H. Sayyad, *J. Optoelectron. Adv. M.* **20**(11-12), 618 (2018).
- [9] F. Zhang, P. Yu, W. Shen, M. Li, R. He, *Comput. Theor. Chem.* **1095**, 118 (2016).
- [10] J. Feng, Y. Jiao, W. Ma, *J. Phys. Chem. C* **117**, 3772 (2013).
- [11] F. Odobel, L. Le Pleux, Y. Pellegrin, E. Blart, *Acc. Chem. Res.* **43**, 1063 (2010).
- [12] M. J. Frisch, G. W. Trucks, H. B. Schlegel, G. E. Scuseria, M. A. Robb, J. R. Cheeseman, G. Scalmani, V. Barone, B. Mennucci, G. A. Petersson, H. Nakatsuji, M. Caricato, X. Li, H. P. Hratchian, A. F. Izmaylov, J. Bloino, G. Zheng, J. L. Sonnenberg, M. Hada, M. Ehara, K. Toyota, R. Fukuda, J. Hasegawa, M. Ishida, T. Nakajima, Y. Honda, O. Kitao, H. Nakai, T. Vreven, J. A. Montgomery, Jr., J. E. Peralta, F. Ogliaro, M. Bearpark, J. J. Heyd, E. Brothers, K. N. Kudin,

- V. N. Staroverov, R. Kobayashi, J. Normand, K. Raghavachari, A. Rendell, J. C. Burant, S. S. Iyengar, J. Tomasi, M. Cossi, N. Rega, J. M. Millam, M. Klene, J. E. Knox, J. B. Cross, V. Bakken, C. Adamo, J. Jaramillo, R. Gomperts, R. E. Stratmann, O. Yazyev, A. J. Austin, R. Cammi, C. Pomelli, J. W. Ochterski, R. L. Martin, K. Morokuma, V. G. Zakrzewski, G. A. Voth, P. Salvador, J. J. Dannenberg, S. Dapprich, A. D. Daniels, O. Farkas, J. B. Foresman, J. V. Ortiz, J. Cioslowski, D. J. Fox, Gaussian 09, Revision A.02. Gaussian, Inc., Wallingford CT, (2009).
- [13] A. Mahmood, M. H. Tahir, A. Irfan, A. G. Al-Sehemi, M. S. Al-Assiri, *Comput. Theor. Chem.* **94**, 1066 (2015).
- [14] J. Tomasi, B. Mennucci, R. Cammi, *Chem. Rev.* **105**, 2999 (2005).
- [15] J. Cui, J. Lu, X. Xu, K. Cao, Z. Wang, G. Alemu, H. Yuang, Y. Shen, J. Xu, Y. Cheng, M. Wang, *J. Phys. Chem. C* **118**, 16433 (2014).
- [16] L. Zhu, H. Yang, C. Zhong, C. M. Li, *Chem. Asian J.* **7**, 2791 (2012).

*Corresponding authors: xiaqiying@163.com;
xhju@njust.edu.cn